

1 ***Supplementary Information***

2

3 **Triptonide-mediated PTGS2 Inhibition Induces Autophagic Cell Death to**
4 **Suppress the Progression of Triple-negative Breast Cancer and Epithelial**
5 **Ovarian Cancer**

6

7 Gong *et al.*

8

9 Scientific Research Center, First School of Clinical Medicine, The First Affiliated
10 Hospital of Guangdong Pharmaceutical University, Guangzhou, 510080, China

11

12 *Correspondence:

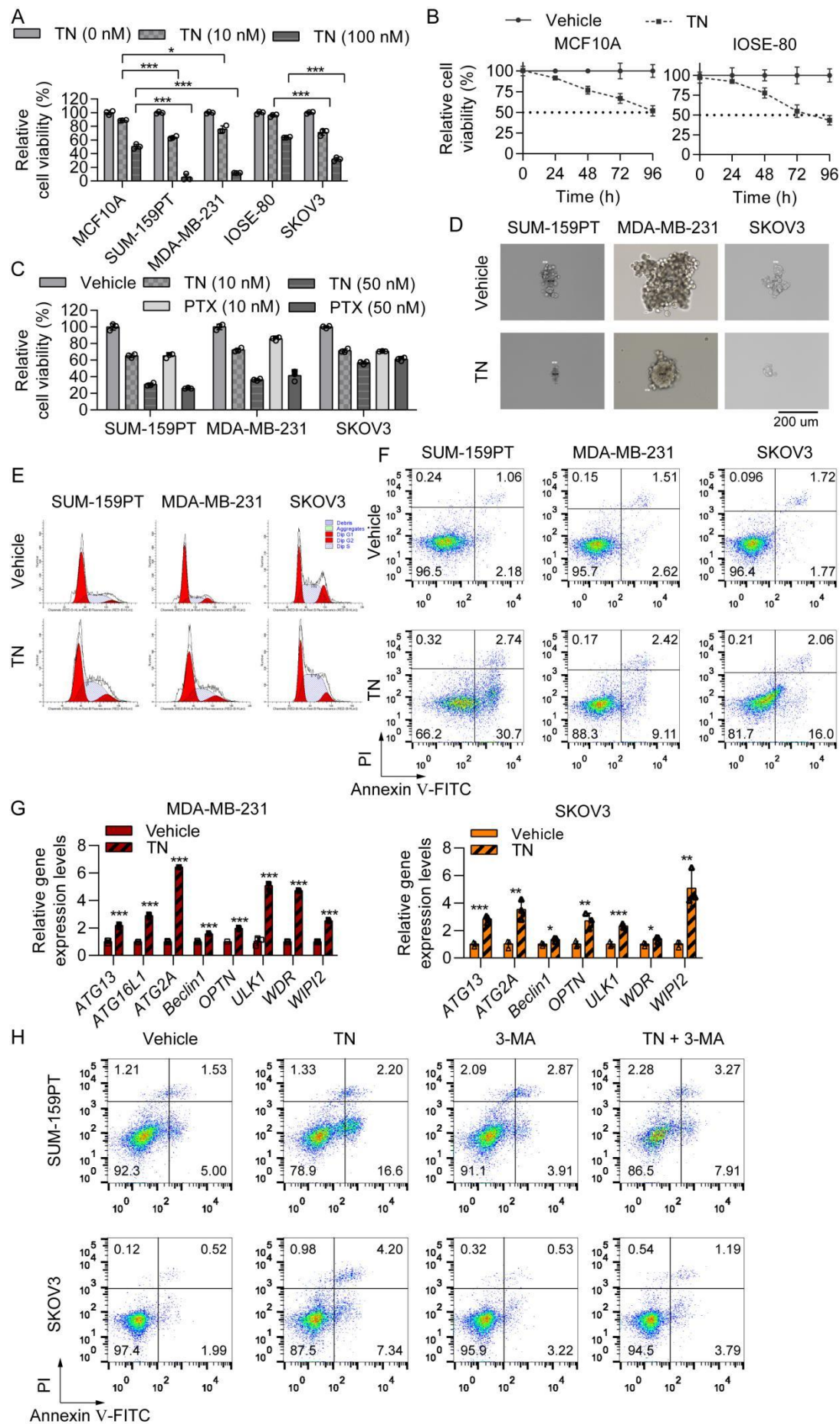
13 Yinger Huang, E-mail: hyeyb@smu.edu.cn

14 Zhe-Sheng Chen, E-mail: chenz@stjohns.edu

15 Wenbo Hao, E-mail: haowa@126.com

16

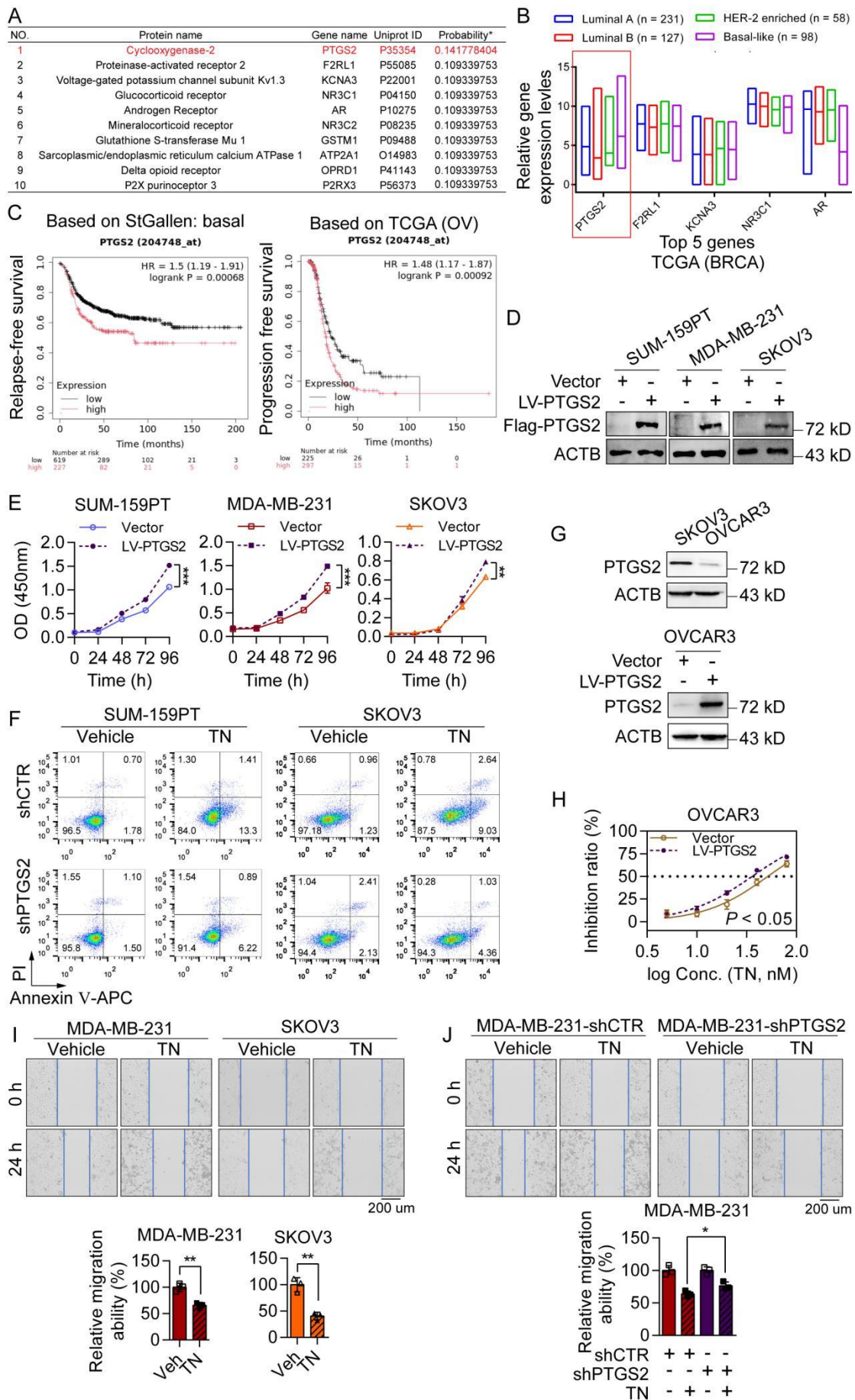
17 **Supplementary Figures**



19 **Fig. S1. Triptonide significantly inhibits the proliferation and promotes apoptosis**
20 **of TNBC and EOC cells.**

21 **(A)** MCF10A, SUM-159PT, MDA-MB-231, IOSE-80 and SKOV3 cells were treated
22 with varying concentrations of TN or vehicle, and cell proliferation was evaluated by
23 a CCK-8 assay. **(B)** Growth curves of MCF10A and IOSE-80 cells treated with
24 vehicle control or 40 nM TN at indicated time points, assessed by CCK-8 assay. **(C)**
25 SUM-159PT, MDA-MB-231, and SKOV3 cells were exposed to different
26 concentrations of TN or PTX for 48 h, and cell proliferation was assessed using a
27 CCK-8 assay. **(D)** Tumorsphere formation assay of SUM-159PT, MDA-MB-231, and
28 SKOV3 cells treated with 40 nM TN. Representative images are shown. **(E)** Cell
29 cycle distribution analyzed by flow cytometry in SUM-159PT, MDA-MB-231, and
30 SKOV3 cells after 24 h treatment with 40 nM TN. Representative histograms are
31 displayed. **(F)** Apoptosis detected by flow cytometry in SUM-159PT, MDA-MB-231,
32 and SKOV3 cells following 48 h exposure to 40 nM TN. Representative images are
33 presented. **(G)** qPCR analysis of autophagy pathway-related gene expression in
34 MDA-MB-231 and SKOV3 cells treated with TN for 24 h. **(H)** Apoptosis evaluated
35 by flow cytometry in SUM-159PT and SKOV3 cells pretreated with 5 mM 3-MA for
36 6 h followed by 40 nM TN for 48 h. Representative diagrams are shown. Data are
37 expressed as mean \pm SD, with statistical significance assessed by Student's t-test; * P
38 < 0.05 , ** $P < 0.01$, *** $P < 0.001$.

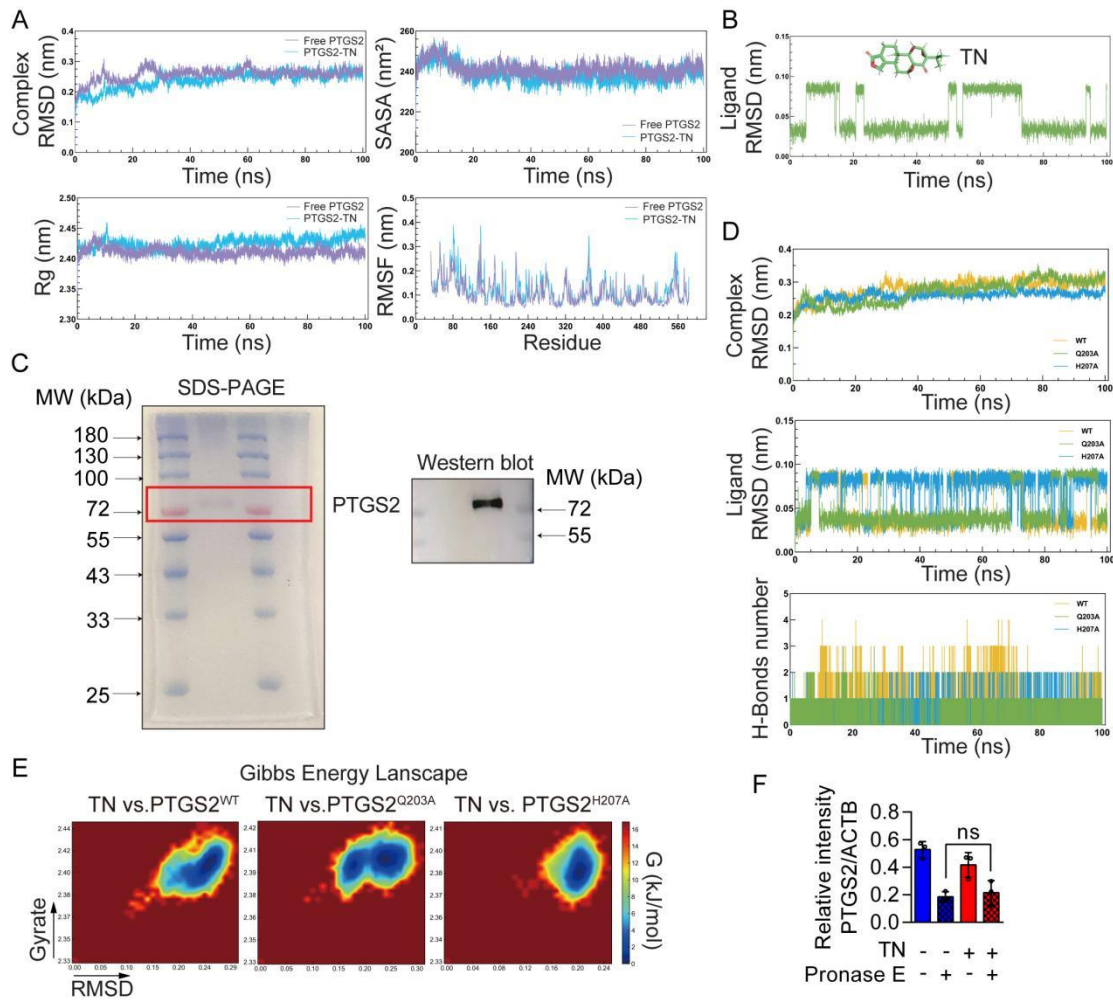
39



41 **Fig. S2. Triptonide targets the PTGS2 protein, which contributes to the**
42 **progression of TNBC and EOC.**

43 **(A)** Potential protein targets of TN. **(B)** mRNA expression levels of the top five
44 potential targets of TN in breast cancer subtypes were analyzed based on the TCGA
45 database. **(C)** Survival analysis of PTGS2 in patients with basal-like breast cancer
46 (*top*) and EOC (*bottom*). **(D)** PTGS2 protein expression levels in vector control and
47 PTGS2-overexpressing SUM-159PT, MDA-MB-231, and SKOV3 cells. **(E)** Growth
48 rates of vector control and PTGS2-overexpressing SUM-159PT, MDA-MB-231, and
49 SKOV3 cells were assessed by CCK-8 assay. **(F)** Apoptosis in TN-treated shRNA
50 control and *PTGS2*-knockdown SUM-159PT and SKOV3 cells after 48 h was
51 evaluated by flow cytometry. Representative diagrams are shown. **(G)** PTGS2 protein
52 expression levels in SKOV3 and OVCAR3 cells (*top*) and in vector control and
53 PTGS2-overexpressing OVCAR3 cells (*bottom*) were assessed by western blot
54 analysis. **(H)** IC₅₀ curves of TN in vector control versus PTGS2-overexpressing
55 OVCAR3 cells. **(I)** Following 24 h treatment with 40 nM TN, changes in the
56 migratory capacity of MDA-MB-231 and SKOV3 cells are shown as representative
57 images (*top*) and corresponding statistical results (*bottom*). **(J)** The migratory ability
58 of *PTGS2*-knockdown and shRNA control MDA-MB-231 cells after 24 h treatment
59 with 40 nM TN. The representative images (*top*) and the corresponding statistical
60 results (*bottom*) are shown. Data are reported as mean \pm SD, with statistical
61 significance evaluated via Spearman's correlation analysis, two-way ANOVA, or
62 Student's t-test; **P* < 0.05, ***P* < 0.01, ****P* < 0.001.

63

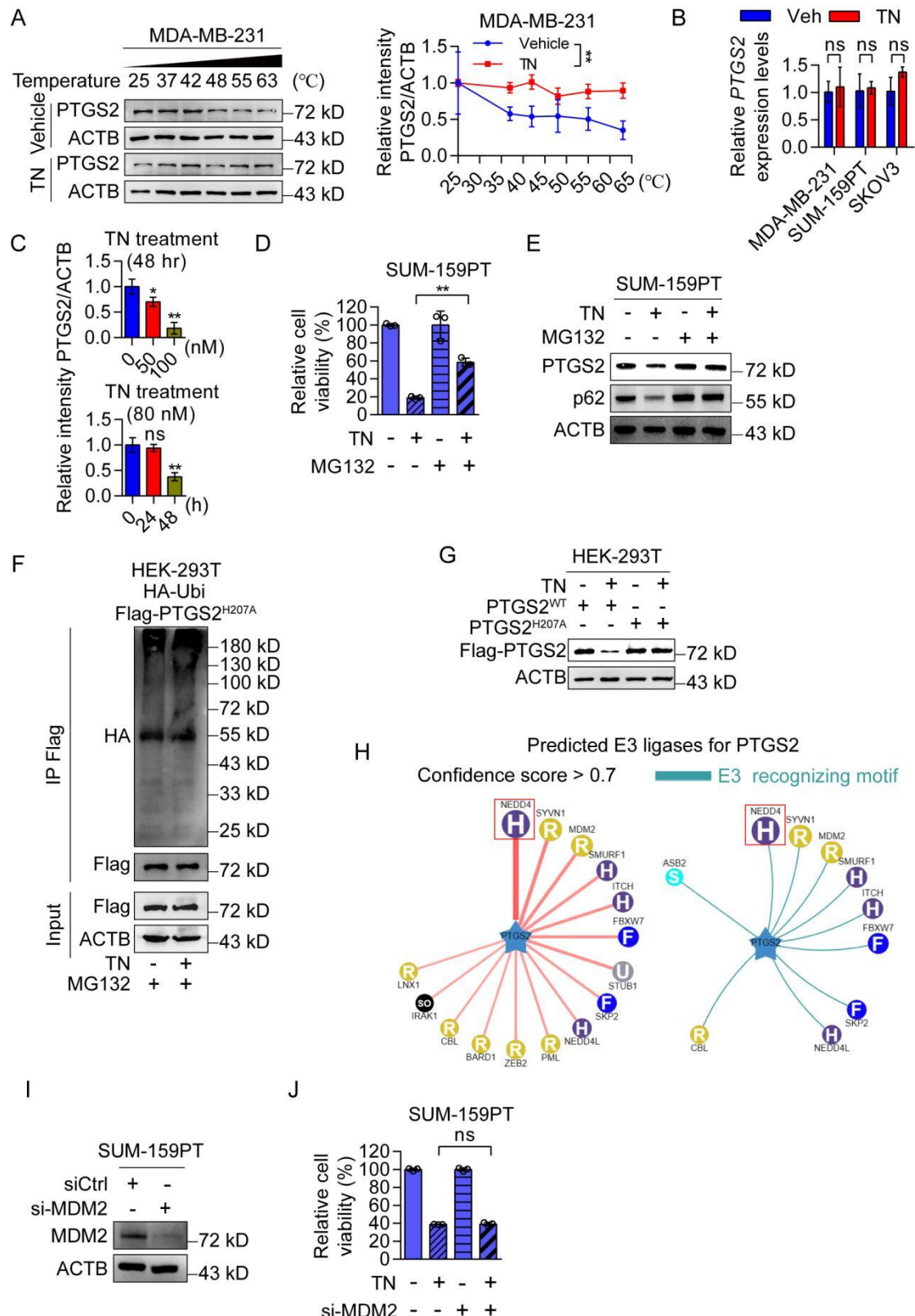


64

65 **Fig. S3. Triptolide exerts anticancer bioactivity by directly binding to His-207 of**
 66 **the PTGS2 protein.**

67 **(A)** Root mean square deviation (RMSD), radius of gyration (Rg), solvent accessible
 68 surface area (SASA), and root mean square fluctuation (RMSF) curves of free PTGS2
 69 and PTGS2-TN complex. **(B)** Fluctuation trajectory of TN in the PTGS2-TN complex.
 70 **(C)** Purified PTGS2 protein detected by coomassie brilliant blue staining and western
 71 blot. **(D)** RMSD curves of PTGS2^{WT/Q203A/H207A}-TN systems, fluctuation trajectory of
 72 TN in PTGS2^{WT/Q203A/H207A}-TN complex, and hydrogen bond number variations in
 73 PTGS2^{WT/Q203A/H207A}-TN systems. **(E)** Two-dimensional Gibbs free energy landscape

74 of TN binding to PTGS2^{WT}, PTGS2^{Q203A}, and PTGS2^{H207A} proteins. (F) Degradation
75 of PTGS2^{H207A} mutant protein in TN-treated cell lysate under pronase E treatment,
76 detected by western blot. Quantitative analysis are shown. Data are expressed as mean
77 \pm SD, with statistical significance assessed by Student's t-test; ns, no significance.
78

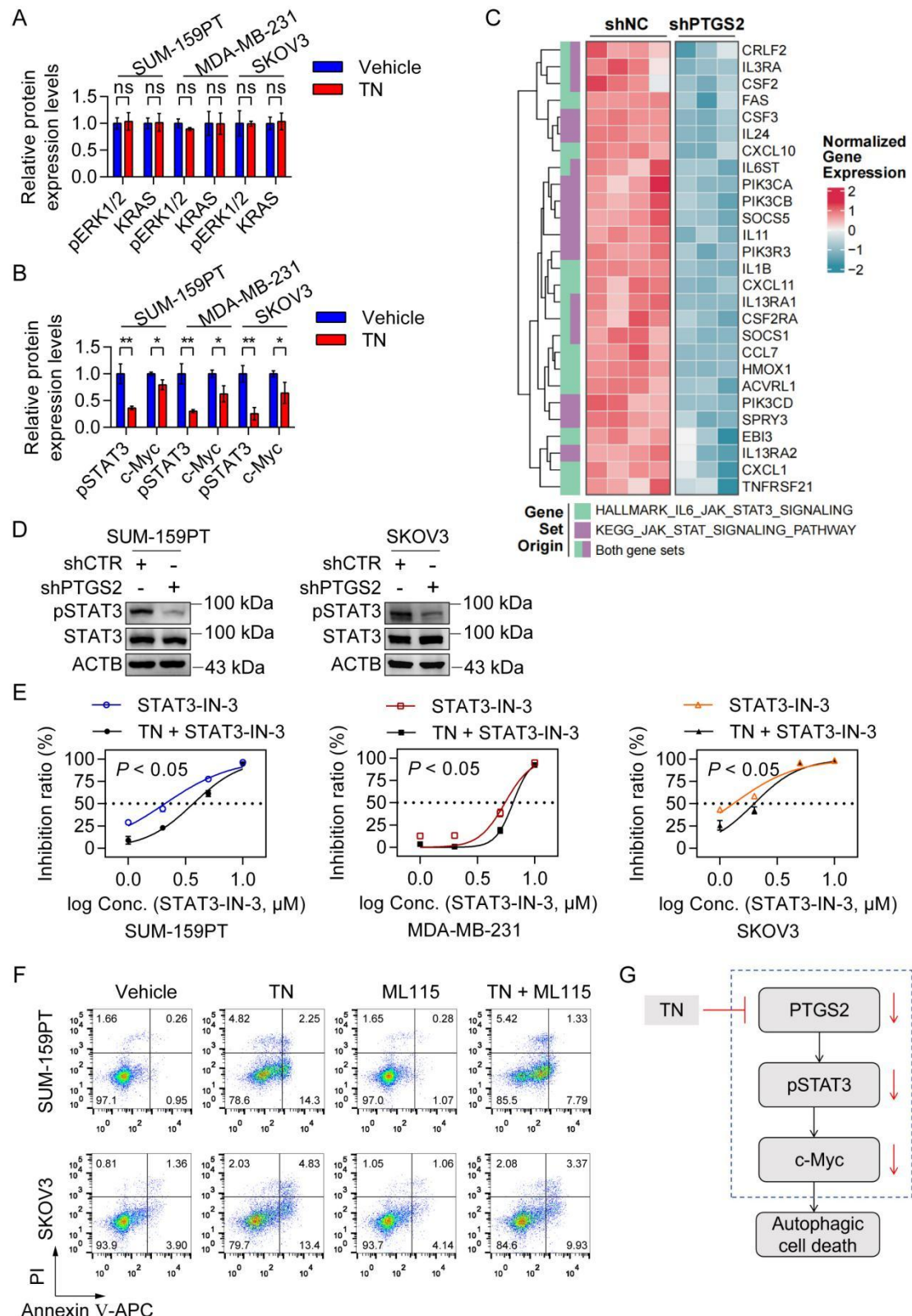


79

80 **Fig. S4. Triptenide promotes PTGS2 degradation via the ubiquitin-proteasome**
81 **system by recruiting the E3 ligase NEDD4.**

82 (A) MDA-MB-231 cell lysate treated with TN was subjected to CETSA assay.
83 Representative blot (*left*) and quantitative analysis (*right*) are shown. (B) qPCR
84 analysis of *PTGS2* gene expression levels in TN-treated SUM-159PT, MDA-MB-231,
85 and SKOV3 cells. (C) Western blot was performed to detect the evaluate the
86 inhibitory effect of TN on *PTGS2* protein expression. Quantitative analysis are shown.
87 (D) SUM159-PT cells were pretreated with MG132 followed by 80 nM TN for 24 h,
88 and cell viability was assessed using the CCK-8 assay. (E) SUM159-PT cells were
89 pretreated with MG132 and then treated with 40 nM TN for 48 h. Protein expression
90 levels of *PTGS2* and p62 were detected by western blot. (F) HEK-293T cells co-
91 expressing *PTGS2*^{H207A} and ubiquitin were pretreated with MG132, followed by
92 treatment with 50 nM TN for 24 h, and the ubiquitination pattern of *PTGS2*^{H207A}
93 protein was assessed by co-IP assay. (G) Western blot analysis was performed to
94 evaluate the inhibitory effect of TN on wild-type and H207-mutated *PTGS2* protein
95 expression. (H) The E3 ubiquitin ligase mediating *PTGS2* ubiquitination was
96 predicted using UbiBrowser v2. (I) Western blot analysis of MDM2 knockdown
97 efficiency. (J) CCK-8 assay was performed to assess the effect of MDM2 knockdown
98 on TN-induced cytotoxicity. Data are reported as mean \pm SD, with statistical
99 significance evaluated via Spearman's correlation analysis, two-way ANOVA, or
100 Student's t-test; * P < 0.05, ** P < 0.01, ns, no significance.

101



102 **Fig. S5. Triptonide induces autophagic cell death by downregulating the**
 103 **JAK/STAT3 signaling pathway.**

104 (A) Quantitative analysis of phosphorylated ERK and KRAS protein levels in SUM-

106 159PT, MDA-MB-231, and SKOV3 cells treated with TN. **(B)** Quantitative analysis
107 of phosphorylated STAT3 and c-Myc protein levels in SUM-159PT, MDA-MB-231,
108 and SKOV3 cells after TN treatment. **(C)** Expression of genes associated with
109 Hallmark-IL6-JAK-STAT3 and KEGG-JAK-STAT signaling pathways in shRNA
110 control and *PTGS2*-knockdown SUM-159PT cells. **(D)** Western blot analysis of
111 pSTAT3 expression in SUM-159PT and SKOV3 cells transduced with shRNA control
112 or *PTGS2*-targeting shRNA. **(E)** SUM-159PT, MDA-MB-231, and SKOV3 cells were
113 pretreated with TN for 12 h, exposed to gradient concentrations of STAT-IN-3 for 24 h,
114 and cell viability was assessed by CCK-8 assay. **(F)** Apoptosis detected by flow
115 cytometry in SUM-159PT and SKOV3 cells treated with TN following ML115
116 administration. Representative diagrams are shown. **(G)** Schematic diagram of TN-
117 mediated autophagic cell death in tumor cells. Data are reported as mean \pm SD, with
118 statistical significance evaluated via Spearman's correlation analysis, two-way
119 ANOVA, or Student's t-test; * P < 0.05, ** P < 0.01, ns, no significance.

120

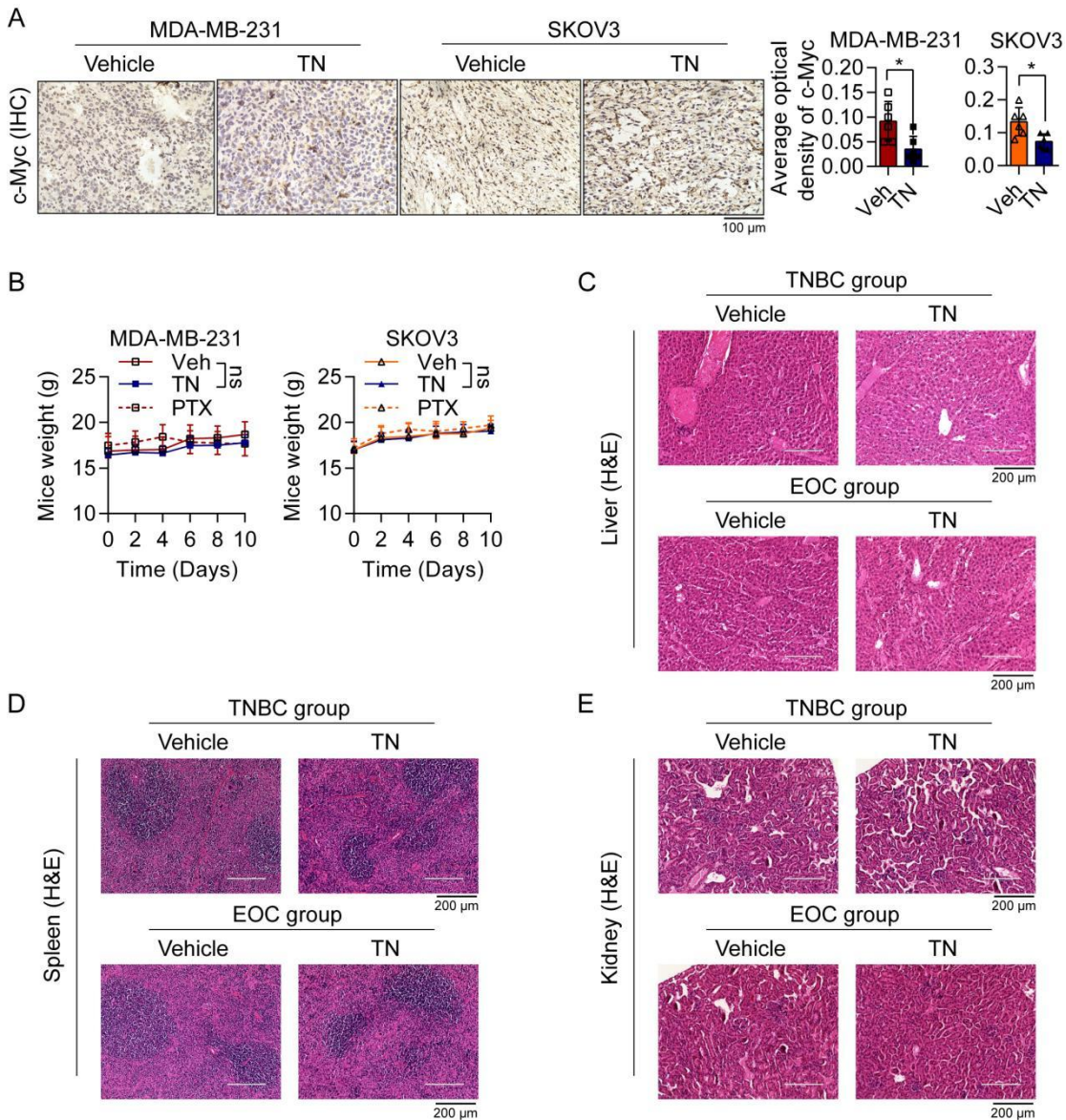


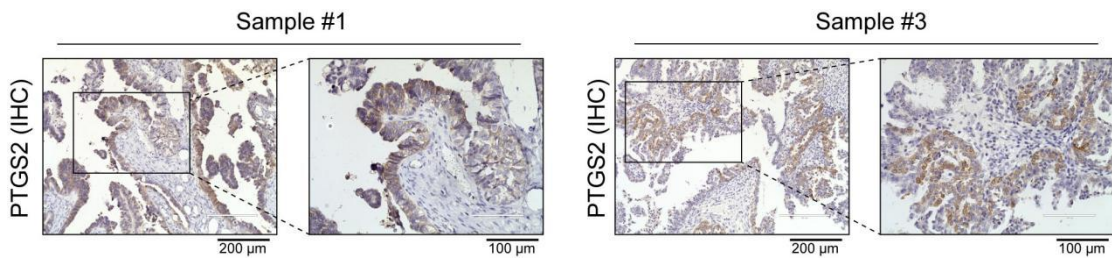
Fig. S6. Triptonide suppresses the growth of TNBC and EOC tumors *in vivo*.

122 (A) IHC staining of c-Myc expression in vehicle-treated and TN-treated groups.
 123 Representative images (*left*) and quantitative analysis are shown (*right*). (B) Body
 124 weight comparison across all experimental mouse groups. (C-E) H&E staining of
 125 important organs (liver, spleen, kidney) from vehicle-treated and TN-treated mice.
 126 Representative images are displayed for liver (C), spleen (D), and kidney (E). Data
 127 are reported as mean \pm SD, with statistical significance evaluated via Spearman's
 128 correlation analysis, two-way ANOVA, or Student's t-test; * P < 0.05, ns, no
 129 correlation.

130 significance.

131

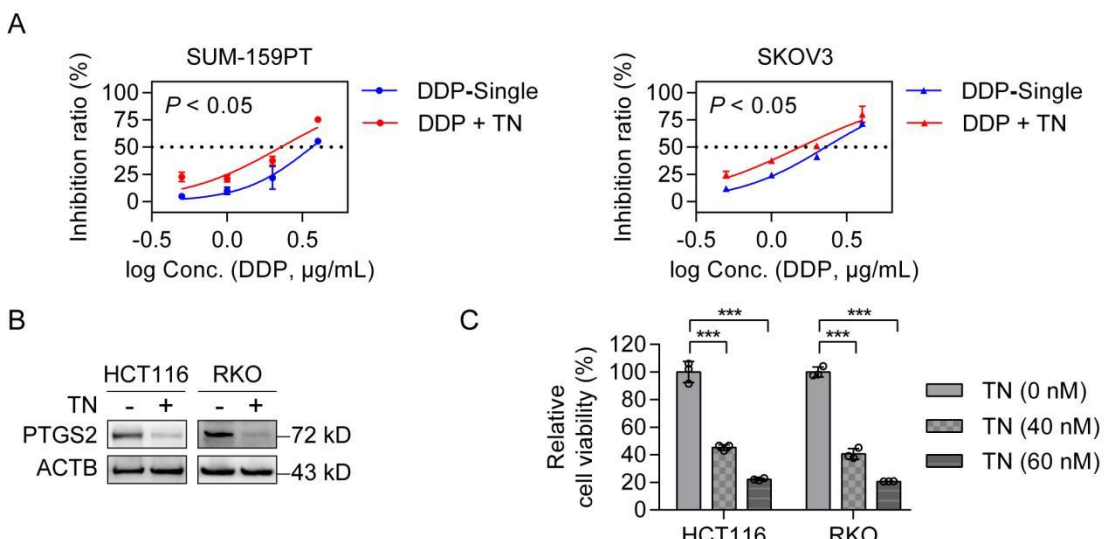
132



133 **Fig. S7. Triptonide suppresses EOC tumorigenesis in PDO models.**

134 IHC staining of PTGS2 expression in tumor tissue samples from patients with EOC,
135 which were used for establishing PDO #1 and #3.

136



137

138 **Fig. S8. TN-mediated chemosensitizing effect and cytotoxicity against colorectal
139 cancer cells.**

140 **(A)** IC₅₀ curves for SUM159-PT and SKOV3 cells following treatment with DDP
141 and/or TN (40 μM) for 48 h. **(B)** Western blot analysis of PTGS2 protein levels in
142 HCT116 and RKO cells treated with DMSO or 40 nM TN for 48 h. **(C)** HCT116 and
143 RKO cells were treated with varying concentrations of TN (0, 40, 60 nM) for 48 h,

144 and cell proliferation was evaluated by a CCK-8 assay. Data are reported as mean ±
145 SD, with statistical significance evaluated via Spearman's correlation analysis, two-
146 way ANOVA, or Student's t-test; *** $P < 0.001$.

147

148 **Supplementary Tables**

149 **Table S1. Sequences used in this study.**

Sequencse name	Sequence (5'-3')
shCTR	CCGGTCCTAAGGTTAAGTCGCCCTCGCTCGAGCGAGGGCGACTAACCTAGGTTTTGAATT
sh- <i>PTGS2</i>	CCGGCTATCACTCAAACGTAAATTCTCGAGAATTTCAGTTGAAGTGATAGTTTTGAATT
siCtrl	UUCUCCGAACGUGUCACGUdTdT
si- <i>NEDD4</i>	CGUUCAGUCUCAAGAAAGATT
si- <i>MDM2</i>	CGCCACAAAUCUGAUAGUAUU

150

151 **Table S2. Primers used in this study.**

Gene	Forward Primers	Reverse Primers
<i>GAPDH</i>	5' -TCTGACTTCAACAGCGACAC-3'	5' -CGTTGTCATACCAGGAAATGAG-3'
<i>ATG13</i>	5' -TCACTTGTGGACCCTGCTTA-3'	5' -TGGTACACACTTCTTGAGAGTCT-3'
<i>ATG16L1</i>	5' -GGAGCTGGCCTGTGTTATGG-3'	5' -GTGACATGTGGTCGGAGAA-3'
<i>ATG2A</i>	5' -TGTCCCTGTAGCCATGTTCTG-3'	5' -TCAGGATCTCCGTGTACTCAG-3'
<i>Beclin 1</i>	5'-AACCTTCCACATCTGGCACA-3'	5'-TCCGTAAGGAACAGTCGGTA-3'

<i>OPTN</i>	5' -CCAAACCTGGACACGTTACC-3'	5' -CCTCAAATCTCCCTTCATGGC-3'
<i>ULK1</i>	5' -GGCAAGTTCGAGTTCTCCCG-3'	5' -CGACCTCCAAATCGTGCTTCT-3'
<i>WDR45</i>	5' -GAGAAGCAACTGCTAGTGTTCC-3'	5' -GGCTGGTTAGAGACACACAG-3'
<i>WIPI2</i>	5' -CCATCGTCAGCCTTAAAGCAC-3'	5' -TCCAGGCATACTATCAGCCTC-3'
<i>PTGS2</i>	5' -CTCCCTGGGTGTCAAAGGTAAA-3'	5' -AACTGATGCGTGAAGTGCTG-3'
<i>MYC</i>	5' -GTAGTGGAAAACCAGCCTCCC-3'	5' -CGTCGCAGTAGAAATACGGCT-3'
